THE NATURE OF THE BRIGHT ULX X-2 IN NGC 3921: A *CHANDRA* POSITION AND *HST* CANDIDATE COUNTERPART

P. G. JONKER[1,2,3], M. HEIDA[1,2], M. A. P. TORRES[1,3], J. C. A. MILLER-JONES[4], A. C. FABIAN[5],
E. M. RATTI[1], G. MINIUTTI[6], D. J. WALTON[5], AND T. P. ROBERTS[7]

[1] SRON, Netherlands Institute for Space Research, Sorbonnelaan 2, 3584 CA Utrecht, The Netherlands; p.jonker@sron.nl
[2] Department of Astrophysics/IMAPP, Radboud University Nijmegen, P.O. Box 9010, 6500 GL Nijmegen, The Netherlands
[3] Harvard-Smithsonian Center for Astrophysics, 60 Garden Street, Cambridge, MA 02138, USA
[4] International Centre for Radio Astronomy Research, Curtin University, GPO Box U1987, Perth, WA 6845, Australia
[5] Institute of Astronomy, Madingley Road, Cambridge CB3 0HA, UK
[6] Centro de Astrobiología (CSIC-INTA), Departamento de Astrofísica, ESA, P.O. Box 78, E-28691 Villanueva de la Cañada, Madrid, Spain
[7] Department of Physics, Durham University, South Road, Durham DH1 3LE, UK

ABSTRACT

We report on *Chandra* observations of the bright ultraluminous X-ray (ULX) source in NGC 3921. Previous *XMM-Newton* observations reported in the literature show the presence of a bright ULX at a 0.5–10 keV luminosity of 2×10^{40} erg s^{-1}. Our *Chandra* observation finds the source at a lower luminosity of $\approx 8 \times 10^{39}$ erg s^{-1}; furthermore, we provide a *Chandra* position of the ULX accurate to $0\rlap{.}''7$ at 90% confidence. The X-ray variability makes it unlikely that the high luminosity is caused by several separate X-ray sources. In three epochs of archival *Hubble Space Telescope* observations, we find a candidate counterpart to the ULX. There is direct evidence for variability between the two epochs of WFPC2 F814W observations with the observation obtained in 2000 showing a brighter source. Furthermore, converting the 1994 F336W and 2000 F300W WFPC2 and the 2010 F336W WFC3 observations to the Johnson *U*-band filter assuming a spectral type of O7I, we find evidence for a brightening of the *U*-band light in 2000. Using the higher resolution WFC3 observations, we resolve the candidate counterpart into two sources of similar color. We discuss the nature of the ULX and the probable association with the optical counterpart(s). Finally, we investigate a potential new explanation for some (bright) ULXs as the decaying stages of flares caused by the tidal disruption of a star by a recoiled supermassive black hole. However, we find that there should be at most only one of such systems within $z = 0.08$.

Key words: binaries: close – X-rays: binaries

1. INTRODUCTION

Ultraluminous X-ray sources (ULXs) are off-nuclear X-ray point sources in nearby galaxies with X-ray luminosities, $L_X \gtrsim 1 \times 10^{39}$–$10^{42}$ erg s^{-1} (Colbert & Mushotzky 1999; Farrell et al. 2009). Their X-ray luminosities are suggestive of intermediate-mass (10^2–10^5 $M_\odot$) black holes (IMBHs) if they radiate isotropically at sub-Eddington levels as observed in stellar black holes and active galactic nuclei (AGNs). Hence, ULXs could be a new kind of black hole with masses in between the stellar-mass black holes found in X-ray binaries and the supermassive black holes (SMBHs; $\gtrsim 1 \times 10^6$ $M_\odot$) found in the centers of galaxies. These IMBHs could be the building blocks of SMBHs (e.g., Volonteri 2010). For a comprehensive overview of ULXs, see Feng & Soria (2011).

Recent studies of the luminosity functions of ULXs and fainter extragalactic X-ray binaries showed evidence for a break at a luminosity $\sim 2 \times 10^{40}$ erg s^{-1} (Swartz et al. 2011; Mineo et al. 2012). This, together with the identification of an ultraluminous spectral state under super-Eddington accretion rarely observed in Galactic black hole X-ray binaries (e.g., Gladstone et al. 2009), led to the idea that the majority of ULXs are stellar-mass black holes. These stellar-mass black holes have particular radiation mechanisms, including beaming effects (King et al. 2001) and/or truly super-Eddington emission (Begelman 2002). Nevertheless, a number of the brightest ULXs with an X-ray luminosity $\gtrsim 2 \times 10^{40}$ erg s^{-1} remain hard to explain as X-ray binaries. The higher the luminosity, the less likely it is that they can be explained as the high-luminosity end of the X-ray binary luminosity function.

A seemingly convincing case for an IMBH is provided by the variable, very bright ULX ESO 243–49 X-1 (Farrell et al. 2009). Its X-ray luminosity is too high for a stellar-mass black hole even in the presence of some beaming. Given the evidence for the detection of a redshifted Hα emission line in the optical counterpart to ESO 243–49 X-1 (Wiersema et al. 2010), the uncertainty on its distance is reduced with respect to other bright ULXs. Another case for an IMBH is M82 X41.4+60; although it does not reach peak luminosities as high as ESO 243–49 X-1, the maximum luminosity is still uncomfortably high for a stellar-mass black hole (Strohmayer & Mushotzky 2003). Feng & Kaaret (2009) showed that M82 X41.4+60 displays state changes similar to those of stellar-mass black holes when at sub-Eddington accretion rates. However, differences in interpretation exist. The temperature of the thermal emission is >1 keV, which is high for an IMBH. Okajima et al. (2006) describe the spectrum as that from a slim disk obtaining a black hole mass of 20–30 $M_\odot$. Similarly, Miyawaki et al. (2009) interpret the thermal emission as coming from a thick corona and find a black hole mass of <200 $M_\odot$.

A further interesting alternative explanation for some (bright) ULXs is that the ULX is caused by a recoiling SMBH in the few million years after the recoil event (Jonker et al. 2010, and references therein). This scenario is not feasible for galaxies where there is evidence for the presence of a central SMBH from, e.g., an AGN. The reason is that the recoiled SMBH

needs to be replaced by a new SMBH in a subsequent merger, and the time for that is longer than the few million years lifetime of the recoiled SMBH as a ULX.

The potential explanation of the ULXs with luminosities above the break in the luminosity function as IMBHs or recoiled SMBHs warrants further investigation of these sources. So far, less than a dozen sources with $L_X \gtrsim 10^{41}$ erg s^{-1} have been found (i.e., in the Cartwheel galaxy, Wolter et al. 2006; M82 X-1, Feng & Kaaret 2009 and Strohmayer & Mushotzky 2003; ESO 243−49, Farrell et al. 2009; NGC 5775, Li et al. 2008; and CXO J122518.6+144545, Jonker et al. 2010). Eight more bright off-nuclear X-ray sources, of which two have $L_X \gtrsim 10^{41}$ erg s^{-1}, were recently reported by Sutton et al. (2012), who suggest that their properties are consistent with accreting IMBHs in the hard state (see Walton et al. 2011).

Here, we present *Chandra*, archival Very Large Array (VLA), and archival *HST*/WFPC2 and *HST*/WFC3 observations of the bright ULX in NGC 3921 first found by Nolan et al. (2004) called NGC 3921 X-2. NGC 3921 is classified as a protoelliptical that was formed during a major merger taking place approximately 0.7 Gyr ago, where one of the merging galaxies was gas rich and the other gas poor (Schweizer 1996; Schweizer et al. 1996). Given that NGC 3921 has an AGN, the recoiling black hole scenario described in Jonker et al. (2010) is not applicable for the ULX under study in this galaxy. We adopt $\Omega_m = 0.3$, $\Omega_\Lambda = 0.7$, and $H_0 = 70$ km s^{-1} Mpc^{-1} to convert the redshift of NGC 3921 to a distance measurement.

2. OBSERVATIONS, ANALYSIS, AND RESULTS

2.1. Chandra X-Ray Observation

We have obtained a 6.0 ks long observation with the *Chandra X-Ray Observatory* (Weisskopf et al. 2002) covering the *XMM-Newton* error circle of the bright ULX in NGC 3921 (Nolan et al. 2004) on 2011 August 14 (MJD 55,787.89362). The *Chandra* observation has been performed using the S3 CCD of the Advanced CCD Imaging Spectrometer (ACIS) detector (Garmire 1997; ACIS-S). The observation identification (ID) number for the data presented here is 13296. We reprocessed and analyzed the data using the CIAO 4.3 software developed by the Chandra X-ray Center and employing CALDB version 4.3. The data telemetry mode was set to *very faint*, which allows for a thorough rejection of events caused by cosmic rays.

Since, by design, the *XMM-Newton* source position falls near the optical axis of the telescope, the size of the point-spread function is smaller than the ACIS pixel size. Therefore, we follow the method of Li et al. (2004) implemented in the CIAO 4.3 tool ACIS_PROCESS_EVENTS to improve the image quality of the ACIS data.

Using WAVDETECT, we have identified the source related to the AGN in NGC 3921 (see Nolan et al. 2004). Using our accurate radio position of the AGN (see below), we apply a boresight correction to the *Chandra* observation of size 0″.155 to the right ascension (R.A.) and −0″.079 to the declination (decl.). For this we used the WCSUPDATE tool inside CIAO. We checked the position of the AGN after the boresight correction, and it matches the radio position to within 0″.02. However, as the radio position is accurate to ∼0″.1, we take the latter as the residual 1σ boresight uncertainty. As the boresight correction involves the position of one source only, we cannot account for effects of rotation.

In the boresight-corrected X-ray image we detect an eight-count X-ray source in the *XMM-Newton* error circle at a position of R.A. = 11:51:07.723 and decl. = +55:04:14.98. In decimal degrees the position, stating in brackets the formal 1σ WAVDETECT uncertainty in localizing the source on the ACIS S3 CCD, is (R.A., decl.) = 177.78218(4), +55.07083(3). The 90% uncertainty in the source position is (R.A., decl.) = (0″.3, 0″.24), with a total uncertainty of 0″.4. This is slightly lower than the uncertainty of 0″.5 (90% confidence) for low-count sources found by Hong et al. (2005), which could potentially be due to the use of the sub-pixel event repositioning that can currently be applied. For the best position we, however, conservatively use an uncertainty of 0″.5 for the uncertainty in localizing the source on the CCD. Given the possibility that the residual boresight correction is due to a systematic effect, we assume, conservatively, that the overall error on the *Chandra* position of the ULX in NGC 3921 is determined by adding the localization uncertainty and the boresight uncertainty (0″.2 at 90% confidence). Overall, the *Chandra* 90% uncertainty on the source position is 0″.7. The source is detected 0″.3 off-axis on the ACIS S3 CCD.

In order to verify that the source we detect in the *XMM-Newton* error circle is not due to residuals from a cosmic-ray event, we investigated the arrival times of the X-ray photons from the source. Indeed, the arrival times of the X-ray photons do not cluster in time as one would expect for residual emission due to a cosmic-ray event.

We also detect four counts from the source that Nolan et al. (2004) list as NGC 3921 X-3. The best *Chandra* position is (R.A., decl.) = (11:51:03.53, +55:04:50.2), which corresponds to 177.76472(5), 55.08061(6) in decimal degrees, where the digit in between brackets denotes the 1σ WAVDETECT uncertainty in localizing the source on the CCD. We do not detect NGC 3921 X-4, which was also considered a ULX by Nolan et al. (2004). Possibly, the source is variable as well and was below our detection limit. Alternatively, the detection of NGC 3921 X-4 was spurious resulting from the incomplete modeling of the *XMM-Newton* point-spread function (see Read et al. 2011). It was excluded from the catalog from Walton et al. (2011) for that reason.

We have selected a circular region of 6 pixel ($\approx 3''$) radius centered on the source position of NGC 3921 X-2 to extract the source counts in the energy range of 0.3–8 keV. We limited the radius to exclude as much as possible the central parts of the galaxy, where extended emission due to either hot gas or unresolved faint point sources may be present. Similarly, we have used a circular region with a radius of 80 pixels away from any source but on the same S3 ACIS CCD to extract background counts. The net number of background-subtracted source counts is 7.7. From the number of background events and the background area we find that the predicted number of background source photons is less than 0.3. For a model of a power law with index 1.7 and negligible interstellar absorption (Dickey & Lockman 1990 give $N_H = 1.1 \times 10^{20}$ cm^{-2} in the direction of NGC 3921) this yields a 0.3–8 keV flux of 1×10^{-14} erg cm^{-2} s^{-1}. However, given the low number of detected counts, the uncertainty on this value is about a factor of two.

Using standard cosmological parameters, the redshift converts to a distance of 80 Mpc for NGC 3921, which makes the X-ray luminosity in the range 0.3–8 keV $L_X \approx 8 \times 10^{39}$ erg s^{-1}. For comparison the 0.5–10 keV luminosity is the same when assuming a power-law spectral model with an index of 1.7 and the Galactic interstellar extinction given above.
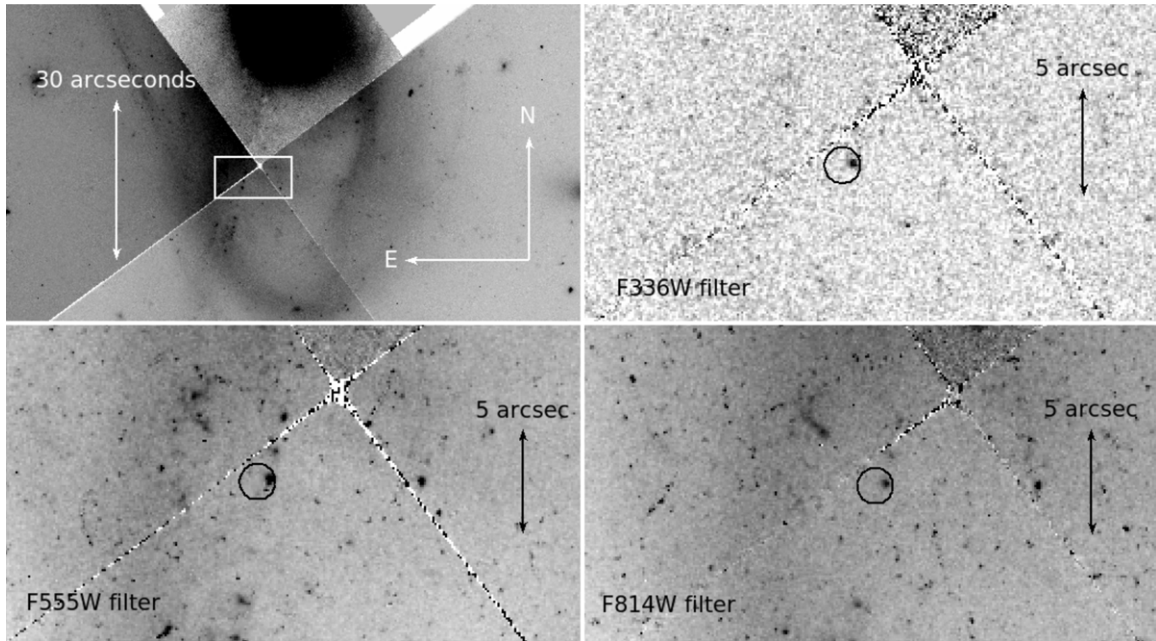
Figure 1. All the images are made using the 1994 WFPC2 observations. The small circle with $0\farcs85$ radius present in three sub-plots represents the 90% confidence astrometric error circle on the position of the ULX. North is up and east is to the left in all panels. Top left panel: overview of the field of NGC 3921 in the F555W filter. The box approximates the size of the small zoomed images. Top right panel: the combined, 1200 s long, *HST* WFPC2 F336W image (*U* band), showing the blue source near the edge of the small circle. Bottom left panel: zoom-in of the combined 2430 s WFPC2 F555W (*V*-band) image around the position of the bright ULX in NGC 3921. Bottom right panel: zoom-in of the combined 1830 s WFPC2 F814W (*I*-band) image around the position of the bright ULX in NGC 3921.

2.2. HST WFPC2 Observations

We have analyzed archival *Hubble Space Telescope* (*HST*) data obtained with the Wide Field Planetary Camera 2 (WFPC2) in the F336W, F555W, and F814W filters corresponding roughly to the Johnson *U*, *V*, and Cousins *I* bands, respectively. We converted the WFPC2 VEGAMAG to the Johnson *U*-, *V*-, and Cousins *I*-band magnitudes using the SYNPHOT package running under STSDAS in IRAF assuming the spectral energy distribution of the O7I star BZ 64. We use this procedure and spectral type for all filter transformations after this. The *HST* data were obtained on 1994 June 28 (MJD 49,623), and the proposal identification number is 5416. Using these *HST* observations, Schweizer et al. (1996) provide the *V*- and *I*-band magnitude (see their Table 3 source number 129) of a source consistent with our *Chandra* X-ray position of NGC 3921 X-2. As we will see below, the *V*- and *I*-band magnitudes of $V = 24.03$ and $I = 24.02$ determined by Schweizer et al. (1996) are fully consistent with the values we derive below using the same *HST* data. We summed the reduced drizzled images provided by the Space Telescope Science Institute giving total exposure times of 2×600 s, 2×1200 s plus 30 s, and 2×900 s plus 30 s for the *U*, *V*, and *I* bands, respectively.

We performed astrometry within *midas*, comparing the positions of stars in the field of view of the WFPC2 against entries from the seventh release of the Sloan Digital Sky Survey (SDSS DR7) r' catalog (Abazajian et al. 2009). An astrometric solution was computed by fitting for the reference point position, the scale, and the position angle, considering all the sources that are not saturated and appear stellar and unblended. We obtain a solution with $0\farcs12$ rms residuals from 15 stars well distributed on the image. The astrometric accuracy of SDSS DR7 is better than 75 mas rms per coordinate, plus 20–30 mas due to systematic errors (Pier et al. 2003). For the accuracy on our stellar positions, we sum in quadrature the residuals of the

astrometry with the rms accuracy of the catalog and add linearly the systematic uncertainty on the SDSS positions. The resulting positional accuracy with respect to the International Celestial Reference System (ICRS) is $0\farcs17$ on both R.A. and decl. at 1σ. The combined *Chandra* and *HST* WFPC2 positional accuracy at 90% confidence is therefore $0\farcs85$ ($0\farcs7$ comes from tying the *Chandra* astrometric frame to the ICRS, see above, and an additional uncertainty of $0\farcs48$ from tying the *HST* frame to the ICRS, adding both in quadrature).

There is a bright point source present inside the 90% confidence astrometric error circle in all three bands at a position R.A. $= 11{:}51{:}07.65$ and decl. $= +55{:}04{:}15.2$ ([R.A., decl.] $= 177.78187(5), +55.07089(5)$ in decimal degrees, where the value in brackets denotes the 1σ uncertainty; see Figure 1). We used sky values determined local to the source of interest as the sky background varies substantially due to a variable amount of unresolved stars of the galaxy. We performed point-spread function fitting for the photometry using the HSTPHOT package (Dolphin 2000). The candidate counterpart present in the summed images gives F336W $= 23.27 \pm 0.15$, F555W $= 23.92 \pm 0.08$, F814W $= 24.01 \pm 0.11$ ($U = 23.7$, $V = 23.9$, $I = 24.0$). The error on the reported photometry is mainly due to spread in aperture correction. As the magnitudes in the *U*, *V*, and *I* bands depend on the spectral type assumed when using SYNPHOT, we do not provide errors for their magnitudes.

Using HSTPHOT, we placed artificial point sources of varying magnitude in the region of 150×150 pixels around the *Chandra* position to determine the limiting magnitude of each of the three combined images separately. We detect point sources at 5σ with F336W < 24.6, F555W < 26.8, F814W < 25.7 ($U < 25.0$, $V < 26.8$, $I < 25.7$). The bright optical source is not resolved in the WFPC2 images although the sharpness parameter from HSTPHOT is at the extreme end of the range for point sources pointing at a nearly resolved source.

Table 1
Results of the Point-spread Function Photometry on the Candidate Optical Counterpart(s) in the Astrometric Error Circle Using Two *HST* WFPC2
(Top Part) and WFC3 (Bottom Part) Observations

Observing Date	Source No.	Time on Source (s)	*HST* Filter Magnitude	Johnson (*UBV*)/Cousins (*I*) Magnitude
1994 Jun 28	1+2	1200	F336W = 23.27 ± 0.15	U = 23.7
1994 Jun 28	1+2	2430	F555W = 23.92 ± 0.08	V = 23.9
1994 Jun 28	1+2	1830	F814W = 24.01 ± 0.11	I = 24.0
2000 Aug 8	1+2	1900	F300W = 22.3 ± 0.1	U = 22.9
2000 Aug 8	1+2	260	F814W = 23.5 ± 0.1	I = 23.5
2010 Oct 3	1	2300	F336W = 23.85 ± 0.03	U = 24.3
2010 Oct 3	2	2300	F336W = 24.27 ± 0.04	U = 24.7
2010 Oct 3	1+2	2300	F336W = 23.29	U = 23.7
2010 Oct 3	1	950	F438W = 23.97 ± 0.05	B = 23.9
2010 Oct 3	2	950	F438W = 24.45 ± 0.07	B = 24.4
2010 Oct 3	1+2	950	F438W = 23.43	B = 23.4

Note. The Johnson and Cousins magnitudes have been calculated using SYNPHOT assuming an O7I spectral type (the star BZ 64).

A second set of *HST* WFC2 observations was obtained on 2000 August 2 using the F300W filter (a wide *U*-band filter) and the F814W filter for total exposure times of 1900 s and 260 s, respectively. Using HSTPHOT, we find that the F300W magnitude of the source is 22.3 ± 0.1, and the F814W magnitude is 23.5 ± 0.1. In both cases the limiting magnitude of the exposures is ≈24. See Table 1 for the conversion of these F300W and F814W magnitudes to Cousins *I* and Johnson *U*-band magnitudes.

2.3. HST WFC3 Observations

In addition to the WFPC2 *HST* observations, we have analyzed archival *HST* data obtained with the Wide Field Camera 3 (WFC3) in the UVIS F336W and the F438W filters. The WFC3 UVIS detector has a pixel scale of 0″.04 per pixel, which is a factor of 2.5 better than that of WFPC2, and 0″.13 per pixel in the infrared (IR) band.

The *HST* WFC3 data were obtained on 2010 October 3 (MJD 55,472), and the proposal identification number is 11691. We summed the reduced drizzled images provided by the Space Telescope Science Institute, giving total exposure times of 2300 s and 950 s for the UVIS F336W and the F438W filters, respectively. Furthermore, we analyzed the observations obtained in the near-infrared F110W- (1565 s in total) and F160W-band exposures (2518 s in total).

We used a procedure similar to the one we used for the WFPC2 images to obtain an accurate astrometric solution for the WFC3 images. We considered all the sources that are not saturated and appear stellar and unblended. Using 11 stars on the F336W-band UVIS image and 7 stars on the near-infrared F110W image for the astrometry, the fit for the reference point position, the scale, and the position angle yielded rms residuals of 0″.05 for the UVIS F336W-band image and 0″.1 for the F110W near-infrared image. The astrometric solution is against the SDSS catalog for the F336W-band UVIS image and against Two Micron All Sky Survey for the near-infrared image. The bright point source present inside the *Chandra* error circle in the WFPC2 images is resolved into two sources in the UVIS images, with positions of R.A. = 11:51:07.647 and decl. = +55:04:15.26 for star 1 and R.A. = 11:51:07.661 and decl. = +55:04:15.36 for star 2 (star 1: [R.A., decl.] = 177.781862(14), +55.070906(14); star 2: [R.A., decl.] = 177.781921(14), +55.070933(14) in decimal degrees, where the value in brackets denotes the 1σ uncertainty; see Figure 2). The

source is unresolved in the near-infrared images. The combined 90% astrometric uncertainty of tying the *HST*/WFC3 images to the ICRS using the SDSS images and of localizing the two stars on the WFC3 optical frames is 0″.3. The total *Chandra* and *HST*/WFC3 combined 90% astrometric uncertainty is therefore 0″.76.

In deriving the photometry of the sources, we used sky values determined local to the source of interest as the sky background varies substantially due to the presence of unresolved stars from the galaxy. We performed point-spread function fitting for the photometry using the DOLPHOT package. The WFC3 magnitudes in the VEGAMAG system for the resolved candidate optical counterpart are given in Table 1. The F336W magnitude of the two sources combined is 23.29. A WFC3 F336W magnitude of 23.29 gives a magnitude of 23.30 for colors similar to those of the O7I star BZ 64 in the WFPC2 F336W filter. This is fully consistent with the magnitude of 23.27 ± 0.15 measured with WFPC2 in its F336W-band filter more than 16 year prior. The combined WFC3 F438W band magnitude of the two sources is 23.43. Converting the WFC3 band magnitudes to Johnson *U*- and *B*-band magnitudes again using the BZ 64 O7I in SYNPHOT, we get U_1 = 24.3 and B_1 = 23.9 and U_2 = 24.7 and B_2 = 24.4 for the F336W and F438W magnitudes of the two sources separately, respectively, and U = 23.7 and B = 23.4 for the two sources combined.

In order to estimate the limiting magnitude of the WFC3 images, we checked the magnitudes of the faintest sources detected at 5σ, and we find approximate limiting magnitudes of F336W < 27.2 and F438W < 26.3 ($U \lesssim 27.6$ and $B \lesssim 26.3$).

3. VLA RADIO OBSERVATIONS

The field of NGC 3921 was observed in the *X* band at a central frequency of 8.4 GHz with the VLA in A-configuration on two occasions in 2003. On 2003 June 19 the source was observed under project code AN114. The source 3C 48 was used as the primary calibrator, and the secondary calibrator was J1146+539. In total the observation provides 14 minutes on target. On 2003 July 14/15 the source was observed under project code AN115. The source 3C 286 was used as the primary calibrator, and the secondary calibrator was J1148+529. In total the observation provides 25 minutes on target.

Data reduction was carried out according to standard procedures within the Astronomical Image Processing System AIPS. The field was not bright enough for self-calibration. When
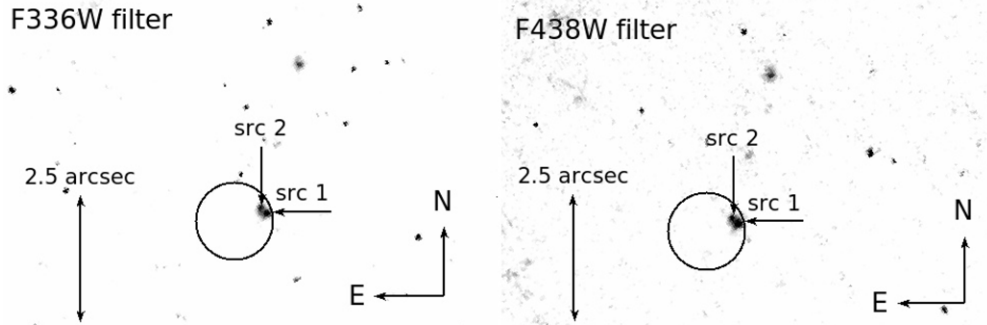
Figure 2. North is up and east is to the left in both panels. Left panel: zoom-in of the combined 2300 s WFC3 F336W image around the position of the bright ULX in NGC 3921. The circle of $0''.76$ radius represents the astrometric 90% confidence region of the position of the ULX. Right panel: zoom-in of the combined, 950 s long, *HST* WFC3 F438W image, showing that the source at the edge of the $0''.76$ radius 90% confidence astrometric error circle is resolved into two sources.

combined, the two observations gave an rms value of the noise of 29 μJy beam^{-1} and no detection at the position of the ULX down to a 3σ upper limit to the radio flux of 87 μJy. This yields a 3σ upper limit on the radio luminosity at the position of the ULX of 5.6×10^{36} erg s^{-1} for a distance of 80 Mpc.

The only significantly detected source corresponds to the center of the galaxy, at R.A. = 11:51:06.8724(2), decl. = 55:04:43.307(2) (J2000), at 1.8 mJy. The errors on those positions are purely statistical. The VLA astrometry is thought to be good to about $0''.1$ in reasonable weather conditions when in A-configuration. Therefore, we have used $0''.1$ as the fiducial 1σ uncertainty on the VLA coordinates of the AGN in NGC 3921.

4. DISCUSSION

We report on a brief *Chandra* observation of the field of the bright ULX in NGC 3921 (Nolan et al. 2004). Compared with the discovery *XMM-Newton* observation $\sim$9.5 years earlier, the source 0.5–10 keV X-ray luminosity has faded by a factor of $\sim$2.5. This virtually proves that the high 0.5–10 keV X-ray luminosity of 2×10^{40} erg s^{-1} detected by *XMM-Newton* is due to a single bright source and not due to the chance super position of a group of sources. If the latter were the case, they, coincidentally, would have decreased their X-ray luminosity by the time of the *Chandra* observation (see Maccarone et al. 2007).

Using the accurate position we obtained using *Chandra*, we investigate archival *HST* WFPC2 images in the F300W, F336W, F555W, and F814W ($2\times$) bands (which we converted to the Johnson U, V, and Cousins I bands, respectively) and archival WFC3 images in the F336W and F438W bands (which we converted to the Johnson U- and B-band magnitudes). There is a single bright, blue optical source in the astrometric error circle in the WFPC2 images. In the WFC3 images this source is resolved into two sources that, when combined, have the same F336W magnitude in the WFC3 and WFPC2 observations of 1994 and 2010 (but see below). With an F336W$-$F438W $= -0.14$, $U - B = 0.3$, and $U - V = -0.2$ color, this source is blue (the color of source 1 and source 2 is approximately equally blue). Furthermore, if at the distance of NGC 3921, with a distance modulus DM of 34.5 excluding extinction effects, its combined absolute V-band magnitude, M_V, is -10.6. The Galactic extinction in the direction of NGC 3921 is found to be 1.1×10^{20} cm^{-2} (Dickey & Lockman 1990). Using the relation of Predehl & Schmitt (1995) between N_H and A_V, we obtain $A_V = 0.06$. Using SYNPHOT, we calculate the F336W$-$F438W color the O7I star BZ 64 would have correcting for extinction. The observed F336W$-$F438W color is too blue to be explained

by the O7I star even if there was no extinction. The color of an O5V star (BZ 77) may be consistent with the observed F336W$-$F438W color if the extinction is slightly lower than the $E(B - V)$ of 0.18 derived from Dickey & Lockman (1990). So, we conclude that the source(s) making up sources 1 and 2 have a combined spectrum similar to that of an early-type star of approximately type O5.

A direct comparison of the two WFPC2 observations employing the F814W filter obtained with just over 6 years in between provides evidence for variability: in 1994 the F814W magnitude was 24.01 ± 0.11, whereas the observation in 2000 found F814W $= 23.5 \pm 0.1$. The *XMM-Newton* observation of Nolan et al. (2004) was obtained on 2002 April 27 when the source was at its highest X-ray luminosity detected so far. The optical observation closest in time to the *XMM-Newton* observation also finds the source at a slightly enhanced luminosity, suggesting that one of the two sources is indeed associated with the X-ray source. Furthermore, comparing the Johnson U-band magnitudes calculated assuming an O7I spectral type, the source is clearly brighter in 2000 than in 1994 and 2010, with U-band magnitudes of 23.7, 22.9, and 23.7 for the observation in 1994, 2000, and 2010, respectively, re-enforcing the evidence for variability.

The optical counterpart is classified as a stellar association or large globular cluster by Schweizer et al. (1996) using the 1994 *HST* WFPC2 observations, as we mentioned in Section 2.2, although they did not consider the U-band observations. In the WFC3 observations, the FWHM of sources 1 and 2 is $\approx$2.4 pixels. This yields an FWHM of $<0''.1$, which at the distance of 80 Mpc of NGC 3921 is about 40 pc for each source. This is on the small side of the size distribution of OB associations (see Bresolin et al. 1998) although the associations in IC 1613 have sizes of 40 pc (Garcia et al. 2010). The $U - V$ color is also consistent with that of young (10–50 Myr old) OB associations (Schulz et al. 2002; Anders & Fritze-v. Alvensleben 2003). In a few nearby ULXs, e.g., NGC 1313 X-2 and Holmberg IX X-1, the age of the surrounding stars is found to be in the same range (Grisé et al. 2008, 2011). Similarly, assuming that one of the optical sources is related to the ULX and the other is an OB cluster, the separation between them is similar to that for M82 X-1 and NGC 7479 found by Voss et al. (2011).

Optical counterparts to ULXs with luminosities below 1×10^{40} erg s^{-1} are typically fainter than the absolute magnitude for NGC 3921 X-2, $M_V = -10.6$. The brightest have $M_V = -9$ (Roberts et al. 2008). The ULXs with higher luminosities are associated with brighter optical counterparts. For instance, the bright ULX in ESO 243$-$49 has $M_R = -10$ (Soria et al.

2010), and the bright ULX in CXO 122518.6+144545 has $M_{g'} = -10.1$ (Jonker et al. 2010). In the following we discuss the possible nature of this bright ULX and the associated potential counterpart.

4.1. NGC 3921 X-2: a ULX with a Stellar-mass Black Hole?

The two candidate optical counterparts to NGC 3921 X-2 are equally blue in the WFC3 observation. Since the accretion disk color can be similarly blue (e.g., van Paradijs & McClintock 1995), perhaps the observed light of one of the sources is dominated by the accretion disk. If so, the other source is dominated by a cluster of stars of a combined color similar to that of the accretion disk. The observed X-ray and optical variability and in particular the large variability in the U-band do suggest that one of the two optical sources identified in the WFC3 images is indeed related to the counterpart to the ULX. If one of the two sources is due to a single object, it could also be a luminous blue variable (LBV; Humphreys & Davidson 1994). If there is evidence that this source is an LBV, it is prudent to assume (Occam's razor) that it will be the mass donor to the accreting black hole in the ULX. The reason is that both LBVs and ULXs are so rare in a galaxy that the probability to find a ULX and an LBV very close together while not physically related is the product of the two (low) probabilities of finding one such source in a certain area in a galaxy.

On the other hand, one may be inclined to assume that evidence for an LBV for one of the two optical sources implies that the other source must be the ULX, reasoning that the number of LBVs in a binary orbit with a black hole must be rarer still than single LBVs. However, most O stars are formed in a binary with another (massive) star (Sana et al. 2012), making the scenario of finding an LBV with a black hole plausible.

Finally, a scenario where both blue optical sources detected in the WFC3 images are young OB clusters is also valid as long as one of them hosts the ULX. When the ULX is X-ray bright, it has to have an optical counterpart of magnitude similar to that of the OB association, explaining the variability. Therefore, the scenario where the ULX in NGC 3921 X-2 is explained as a stellar-mass black hole accreting from a donor in a wide system such that the absolute magnitude of the donor plus disk rivals that of an OB association is entirely consistent with the data.

4.2. NGC 3921 X-2: a Type IIn Supernova?

As the combined U-band magnitude from the WFC3 sources 1 and 2 measured in 2010 is consistent with being the same as the WFPC2 U-band magnitude measured in 1994 while there is evidence for moderate brightening in 2000, a scenario explaining the ULX as a Type IIn supernova (see Gal-Yam & Leonard 2009; Jonker et al. 2010) is strongly constrained. The scenario that still is (theoretically) possible but that we deem unlikely is as follows: the progenitor star of the supernova was not detected; therefore, it should reside in a cluster that is still present. The supernova went off some time between 1994 and 2000 and, remarkably, went undetected in the optical. This includes a non-detection in archival ground-based observations from the Jacobus Kaptein Telescope in 1996. The supernova has faded in the optical before the *HST* observation in 2000 nearly down to the pre-explosion level. The X-rays come from the supernova and are now fading.

4.3. A New Scenario for the Nature of Some ULXs: Tidal Disruption of a Star by a Recoiled Black Hole?

A galaxy like our Milky Way is predicted to have hundreds of recoiled IMBHs/SMBHs with associated star clusters (O'Leary & Loeb 2012). For the majority of systems that are expected to have had recoil velocities <1000 km s^{-1}, the rate of tidal disruption events remains constant for about 1 Gyr after the recoil event. Given the expected rate, one could have about 1000 events in 1 Gyr (Komossa & Merritt 2008). Tidal disruption of stars from such a bound (nuclear) cluster or from unbound stars of the galaxy will produce periods of enhanced accretion providing X-ray luminosities above 10^{40} erg s^{-1} (Komossa & Merritt 2008; Stone & Loeb 2012). The short-duration Eddington-limited flares may well be missed by current scanning X-ray All Sky Monitors, whereas the flares may be too soft to be detected by the *Swift* Burst Alert Telescope instrument (see Lodato & Rossi 2011 for the predicted light curves and the disk temperatures). Theoretically, one expects the timescale of the decay of mass accretion rate to go as $t^{-5/3}$ (Rees 1988; Rees 1990). Recent *Chandra* observations of three potential tidal disruption events are consistent with this theoretical trend and an overall lifetime of approximately 5 years at $L_x > 10^{40}$ erg s^{-1} (Halpern et al. 2004). In order to determine the importance of tidal disruption events from recoiled, off-nuclear black holes for the population of ULXs, we need to estimate the number of such black holes that recoiled in approximately the last Gyr. The rate of tidal disruption events drops off steeply for longer times as the loss cone of the recoiled black hole is emptied (Komossa & Merritt 2008).

Patton et al. (2000) found that over the last 1 Gyr about 1% of galaxies with an absolute B-band magnitude $-21 \leqslant M_B \leqslant -18$ went through a merger (see their formula (32)). This was derived evaluating the number of interacting galaxies found in the Second Southern Sky Redshift Survey. As the authors explain, this fraction is a lower limit as only pairs of relatively bright galaxies have been included. Including fainter galaxies would increase the fraction as more interacting bright + faint galaxy pairs would be found. More recently, De Propris et al. (2007) found a merger fraction of 2% using close pair fractions and asymmetries from the Millennium Galaxy catalog.

Assuming that the black hole merger time is significantly less than 1 Gyr such as in gas-rich mergers (e.g., Mayer et al. 2007) will provide a lower limit on the number of recently (within the last Gyr) recoiled black holes. In the case that this merger time is much longer (of order of several Gyr) the number of recently recoiled black holes is larger as the galaxy merger fraction was high at larger redshift (e.g., Patton et al. 2000; Lin et al. 2004).

In order to derive the number of off-nuclear recoiled black holes that recoiled in approximately the last Gyr, we need to know the fraction of merging black holes that receive a significant kick. This fraction is debated at present. The magnitude of the recoil kick depends on the mass ratio of the two black holes before their merger, on the orientation of their spin axes with respect to the binary orbital plane, and on the amount of spin. The presence of massive gas disks around the binary black hole such as potentially in gas-rich mergers can align the spin axes of the two black holes prior to their merger, reducing the amplitude of the recoil kick imparted during the merger (Bogdanović et al. 2007; Dotti et al. 2010). However, fragmentation of the accretion disk around the binary SMBH could reduce the rate of alignment as fragments could result in short randomly oriented accretion events (King & Pringle

2007). Recent calculations seem to suggest that the recoil kicks might be limited to velocities lower than ≈ 200 km s^{-1} due to a gravitational wave "anti-kick" during the ringdown phase (Le Tiec et al. 2010). Similarly, under certain conditions relativistic precession will align or anti-align the black hole spin vectors, reducing the median kick velocities (Kesden et al. 2010). Recoil velocities of a few hundred km s^{-1} imply that many recoiling SMBHs will be retained by the host galaxy. Too small recoil velocities will mean that the recoiled black hole will sink back to the nucleus of the galaxy and X-ray emission due to decaying tidal disruption events will not be identified as ULXs. For now we assume that 50% of the recoiled black holes will have recoil velocities such that they are bound to the galaxy and that they appear as off-nuclear sources for 1 Gyr. We note, however, that this number depends on the distribution of recoil kick velocities, which is uncertain.

Putting all these estimates together, we calculate the probability of finding a ULX caused by tidal disruption of a star by a recoiled SMBH per galaxy. There is 2% (the merger fraction) × 50% (right recoil velocity) × 1×10^{-6} yr^{-1} (the tidal disruption rate per year) × 5 (the lifetime in years above a luminosity of 1×10^{40} erg s^{-1}) leading to about 5 in 10^8 galaxies that potentially have a bright off-nuclear X-ray source due to the fading of emission caused by a tidal disruption event.

The 1 Gyr look-back time corresponds to a redshift of $z \approx 0.08$. This provides a comoving volume of 0.16 Gpc^{-3}. Given the galaxy density $\phi_\star \approx 1 \times 10^{-2}$ Mpc^{-3} (see Schechter 1976; Loveday et al. 1992; Driver et al. 2005 for $h = 0.7$), there are about 1.6 million galaxies in this volume. Therefore, there will be between 0.1 and 1 X-ray sources with $L > 10^{40}$ erg s^{-1} due to tidally disrupted stars from off-nuclear, recoiled black holes within a redshift of 0.08. Note that a luminosity of $L > 10^{40}$ erg s^{-1} at a redshift of $z = 0.08$ corresponds to a flux of only $\approx 7 \times 10^{-16}$ erg cm^{-2} s^{-1}, making it difficult to detect these sources in the existing shallow surveys. If the estimates above are reasonable, there might be at most one of these among the (bright) ULXs such as the ULX NGC 3921 X-2.

4.3.1. Application to NGC 3921 X-2

The decay in X-ray luminosity of a factor of 2.5 in NGC 3921 X-2 that we find between the *XMM-Newton* and *Chandra* observations ∼3400 days apart is (too) small compared to the predicted drop-off from the soft disk X-ray spectral component predicted by Lodato & Rossi (2011). Even if in some proposed tidal disruption events the X-ray spectrum is found to be significantly harder than expected, the luminosity is about a factor of 200 lower 3165 days after the soft peak (Komossa et al. 2004). Given the presence of nuclear activity in NGC 3921, a new central SMBH must have replaced the recoiled black hole, for instance, following a recent merger, or the recoiled black hole was formed by a three-black-hole interaction event. All these constraints, of course, make the scenario of a tidal disruption event in a recoiled SMBH for NGC 3921 X-2 unlikely.

4.4. Alternative Explanations for NGC 3921 X-2?

Alternative explanations for the bright ULX in NGC 3921 such as a background AGN or a foreground star or (quiescent) low-mass X-ray binary (LMXB) are possible in principle. For NGC 3921 X-2 to be an active LMXB the distance should be ≈ 1 Mpc for a luminosity of 1×10^{36} erg s^{-1} typical for an LMXB. This would give an absolute *V*-band magnitude of around -1, which is in line with that of LMXBs (van Paradijs

& McClintock 1995); however, finding an LMXB in interstellar space is unlikely. NGC 3921 X-2 can also be a quiescent LMXB at a distance of a few kpc. The absolute magnitude of the optical counterpart would then be pointing to an M-type companion, which would imply that the blue candidate optical counterparts have to be unrelated to the quiescent LMXB.

Schweizer et al. (1996) estimate the number of background galaxies in the WFPC2 field of view as 1.2×10^{-3} arcsec^{-2}. The presence of the background galaxy cluster A1400 is taken into account in this estimate. The optical counterpart does coincide spatially with one of the tidal tails that clearly belongs to NGC 3921. As the (young) stellar associations in NGC 3921 trace these tails very well, the probability of finding a background AGN among these stellar associations is low.

In the case that the optical source is unrelated to the X-ray source the observed variability in the F814W (and *U*-band) WFPC2 observations is hard to explain. Nevertheless, assuming that the variability is spurious or explained in another way, we can provide a limit on the absolute magnitude of the counterpart of $M_U > -7.3$, $M_B > -8.2$, $M_V > -7.7$, and $M_I > -8.8$. These limits on M_U, M_B, M_V, and M_I have been derived using the upper limits on the apparent magnitude of <27.2, <26.3, <26.8, and <25.7, respectively, and given the distance of 80 Mpc toward NGC 3921.

Therefore, the source could be a ULX with a stellar counterpart outside an association. The upper limit to an optical source in this scenario translates to a lower limit on the ratio of the X-ray flux to the optical flux of 12. Whereas most *Chandra*-selected AGNs have a ratio of X-ray to optical *R*-band flux of lower than 10 (Laird et al. 2009), our limit does not rule out a background AGN scenario in the case that the optical source is unrelated to the X-ray source. The most secure way to differentiate between the discussed scenarios is to obtain an optical spectrum of the potential counterparts.

REFERENCES

Abazajian, K. N., Adelman-McCarthy, J. K., Agüeros, M. A., et al. 2009, ApJS, 182, 543
Anders, P., & Fritze-v. Alvensleben, U. 2003, A&A, 401, 1063
Begelman, M. C. 2002, ApJ, 568, L97
Bogdanović, T., Reynolds, C. S., & Miller, M. C. 2007, ApJ, 661, L147
Bresolin, F., Kennicutt, R. C., Jr., Ferrarese, L., et al. 1998, AJ, 116, 119
Colbert, E. J. M., & Mushotzky, R. F. 1999, ApJ, 519, 89
De Propris, R., Conselice, C. J., Liske, J., et al. 2007, ApJ, 666, 212

Dickey, J. M., & Lockman, F. J. 1990, ARA&A, 28, 215
Dolphin, A. E. 2000, PASP, 112, 1383
Dotti, M., Volonteri, M., Perego, A., et al. 2010, MNRAS, 402, 682
Driver, S. P., Liske, J., Cross, N. J. G., De Propris, R., & Allen, P. D. 2005, MNRAS, 360, 81
Farrell, S. A., Webb, N. A., Barret, D., Godet, O., & Rodrigues, J. M. 2009, Nature, 460, 73
Feng, H., & Kaaret, P. 2009, ApJ, 696, 1712
Feng, H., & Soria, R. 2011, New Astron. Rev., 55, 166
Gal-Yam, A., & Leonard, D. C. 2009, Nature, 458, 865
Garcia, M., Herrero, A., Castro, N., Corral, L., & Rosenberg, A. 2010, A&A, 523, A23
Garmire, G. P. 1997, BAAS, 29, 823
Gladstone, J. C., Roberts, T. P., & Done, C. 2009, MNRAS, 397, 1836
Grisé, F., Kaaret, P., Pakull, M. W., & Motch, C. 2011, ApJ, 734, 23
Grisé, F., Pakull, M. W., Soria, R., et al. 2008, A&A, 486, 151
Halpern, J. P., Gezari, S., & Komossa, S. 2004, ApJ, 604, 572
Hong, J., van den Berg, M., Schlegel, E. M., et al. 2005, ApJ, 635, 907
Humphreys, R. M., & Davidson, K. 1994, PASP, 106, 1025
Jonker, P. G., Torres, M. A. P., Fabian, A. C., et al. 2010, MNRAS, 407, 645
Kesden, M., Sperhake, U., & Berti, E. 2010, ApJ, 715, 1006
King, A. R., Davies, M. B., Ward, M. J., Fabbiano, G., & Elvis, M. 2001, ApJ, 552, L109
King, A. R., & Pringle, J. E. 2007, MNRAS, 377, L25
Komossa, S., Halpern, J., Schartel, N., et al. 2004, ApJ, 603, L17
Komossa, S., & Merritt, D. 2008, ApJ, 683, L21
Laird, E. S., Nandra, K., Georgakakis, A., et al. 2009, ApJS, 180, 102
Le Tiec, A., Blanchet, L., & Will, C. M. 2010, Class. Quantum Grav., 27, 012001
Li, J., Kastner, J. H., Prigozhin, G. Y., et al. 2004, ApJ, 610, 1204
Li, J., Li, Z., Wang, Q. D., Irwin, J. A., & Rossa, J. 2008, MNRAS, 390, 59
Lin, L., Koo, D. C., Willmer, C. N. A., et al. 2004, ApJ, 617, L9
Lodato, G., & Rossi, E. M. 2011, MNRAS, 410, 359
Loveday, J., Peterson, B. A., Efstathiou, G., & Maddox, S. J. 1992, ApJ, 390, 338
Maccarone, T. J., Kundu, A., Zepf, S. E., & Rhode, K. L. 2007, Nature, 445, 183
Mayer, L., Kazantzidis, S., Madau, P., et al. 2007, Science, 316, 1874

Mineo, S., Gilfanov, M., & Sunyaev, R. 2012, MNRAS, 419, 2095
Miyawaki, R., Makishima, K., Yamada, S., et al. 2009, PASJ, 61, 263
Nolan, L. A., Ponman, T. J., Read, A. M., & Schweizer, F. 2004, MNRAS, 353, 221
Okajima, T., Ebisawa, K., & Kawaguchi, T. 2006, ApJ, 652, L105
O'Leary, R. M., & Loeb, A. 2012, MNRAS, 421, 2737
Patton, D. R., Carlberg, R. G., Marzke, R. O., et al. 2000, ApJ, 536, 153
Pier, J. R., Munn, J. A., Hindsley, R. B., et al. 2003, AJ, 125, 1559
Predehl, P., & Schmitt, J. H. M. M. 1995, A&A, 293, 889
Read, A. M., Rosen, S. R., Saxton, R. D., & Ramirez, J. 2011, A&A, 534, A34
Rees, M. J. 1988, Nature, 333, 523
Rees, M. J. 1990, Science, 247, 817
Roberts, T. P., Levan, A. J., & Goad, M. R. 2008, MNRAS, 387, 73
Sana, H., de Mink, S. E., de Koter, A., et al. 2012, Science, 337, 444
Schechter, P. 1976, ApJ, 203, 297
Schulz, J., Fritze-v. Alvensleben, U., Möller, C. S., & Fricke, K. J. 2002, A&A, 392, 1
Schweizer, F. 1996, AJ, 111, 109
Schweizer, F., Miller, B. W., Whitmore, B. C., & Fall, S. M. 1996, AJ, 112, 1839
Soria, R., Hau, G. K. T., Graham, A. W., et al. 2010, MNRAS, 405, 870
Stone, N., & Loeb, A. 2012, MNRAS, 422, 1933
Strohmayer, T. E., & Mushotzky, R. F. 2003, ApJ, 586, L61
Sutton, A. D., Roberts, T. P., Walton, D. J., Gladstone, J. C., & Scott, A. E. 2012, MNRAS, 423, 1154
Swartz, D. A., Soria, R., Tennant, A. F., & Yukita, M. 2011, ApJ, 741, 49
van Paradijs, J., & McClintock, J. E. 1995, in X-ray Binaries, ed. W. H. G. Lewin, J. van Paradijs, & E. P. J. van den Heuvel (Cambridge: Cambridge Univ. Press), 58
Volonteri, M. 2010, Nature, 466, 1049
Voss, R., Nielsen, M. T. B., Nelemans, G., Fraser, M., & Smartt, S. J. 2011, MNRAS, 418, L124
Walton, D. J., Roberts, T. P., Mateos, S., & Heard, V. 2011, MNRAS, 416, 1844
Weisskopf, M. C., Brinkman, B., Canizares, C., et al. 2002, PASP, 114, 1
Wiersema, K., Farrell, S. A., Webb, N. A., et al. 2010, ApJ, 721, L102
Wolter, A., Trinchieri, G., & Colpi, M. 2006, MNRAS, 373, 1627